HHS Public Access

Author manuscript

J Chromatogr A. Author manuscript; available in PMC 2016 December 04.

Published in final edited form as:

J Chromatogr A. 2015 December 4; 1423: 19–30. doi:10.1016/j.chroma.2015.10.060.

Selective Capture of Glycoproteins Using Lectin-modified Nanoporous Gold Monolith

Allan J. Alla[a,b], **Felipe B. d'Andrea**[a,b], **Jay K. Bhattarai**[a,b], **Jared A. Cooper**[a,b], **Yih Horng Tan**[a,b], **Alexei V. Demchenko**[a], and **Keith J. Stine**[a,b,*]

[a]Department of Chemistry and Biochemistry, One University Boulevard, University of Missouri Saint Louis, Saint Louis, MO USA 63121

[b]Center for Nanoscience, One University Boulevard, University of Missouri Saint Louis, Saint Louis, MO USA 63121

Abstract

The surface of nanoporous gold (np-Au) monoliths was modified via a flow method with the lectin Concanavalin A (Con A) to develop a substrate for separation and extraction of glycoproteins. Self-assembled monolayers (SAMs) of lipoic acid (LA) on the np-Au monoliths were prepared followed by activation of the terminal carboxyl groups to create amine reactive esters that were utilized in the immobilization of Con A. Thermogravimetric analysis (TGA) was used to determine the surface coverages of LA and Con A on np-Au monoliths which were found to be 1.31×10^{18} molecules m^{-2} and 1.85×10^{15} molecules m^{-2}, respectively. An in situ solution depletion method was developed that enabled surface coverage characterization without damaging the substrate and suggesting the possibility of regeneration. Using this method, the surface coverages of LA and Con A were found to be 0.989×10^{18} molecules m^{-2} and 1.32×10^{15} molecules m^{-2}, respectively. The selectivity of the Con A-modified np-Au monolith for the high mannose-containing glycoprotein ovalbumin (OVA) versus negative control non-glycosylated bovine serum albumin (BSA) was demonstrated by the difference in the ratio of the captured molecules to the immobilized Con A molecules, with OVA:Con A = 2.3 and BSA:Con A = 0.33. Extraction of OVA from a 1:3 mole ratio mixture with BSA was demonstrated by the greater amount of depletion of OVA concentration during the circulation with the developed substrate. A significant amount of captured OVA was eluted using α-methyl mannopyranoside as a competitive ligand. This work is motivated by the need to develop new materials for chromatographic separation and extraction substrates for use in preparative and analytical procedures in glycomics.

Keywords

nanoporous gold; chromatography; lectin; glycoprotein; monolith; glycomics

*Corresponding Author: Phone: (314)516-5346, Fax: (314)516-5342, kstine@umsl.edu.

1. Introduction

Glycoproteins have attached oligosaccharide units called glycans, and belong to the collective group known as glycoconjugates. They are formed as a result of the post-translational modification of proteins in which glycans are covalently attached to an amino acid sequence, with N-linked or O-linked glycans being the most prevalent. Glycans on the cell surface serve as the recognition armies of cells, a function that is essential in cell-to-cell adhesion and recognition [1,2]. Another significant role of glycans is their role in the conformational changes that glycoproteins must undergo in order to perform specific biological functions [3]. Aberrant glycosylation, i.e., changes in oligosaccharide structure upon biosynthesis can be related to diseases such as cancer [4]; therefore, glycoproteins are now used as cancer biomarkers [5,6].

The study of glycans and their structures and functions is called glycomics. Unlike proteins or polynucleotides, the structures of glycans are complex, heterogeneous and isobaric. This poses a challenge in glycomics where elucidation and identification of glycan structure and the glycosylation sites of glycopeptides are required in determining their respective biological functions [7]. Various methods are used in glycan analysis such as mass spectrometry (MS) [8–10], nuclear magnetic resonance (NMR) [11], electrochemistry [12], UV detection of derivatized glycans [13] and fluorescence imaging [14]. Comprehensive glycan analysis using microarrays of lectins [15] and antibodies [16] has also been developed. Prior to analysis, several preparative methods are usually needed that may include separation, isolation and enrichment in order to increase the abundance of glycoproteins, glycopeptides and glycans in complex samples such as serum, plant and cell tissue extracts and cultured cells. Preparative methods in glycomics include sodium dodecyl sulfate polyacrylamide gel electrophoresis (SDS-PAGE) [17], capillary electrophoresis (CE) [18] and chromatographic separation methods such as liquid chromatography (LC) [19] and capillary electrochromatography (CEC) [20].

One major factor that determines the success and efficiency of chromatographic separation is the optimization of the stationary phases in which different ligands are attached to a matrix or substrate that can selectively capture and isolate target analytes. In separation of intact glycoproteins, a popular and widely used method is lectin affinity chromatography (LAC). Lectins are proteins that contain carbohydrate-binding domains that bind with specificity to glycan structures of glycoproteins [21]. The binding is reversible and ligands can be displaced by competition or by changing the conditions of the mobile phase such as pH and ionic strength. Lectins are classified by their sequence similarity and structural organization. Lis and Sharon proposed five groups according to the monosaccharide for which the lectin exhibits the highest affinity: (1) mannose (2) galactose/*N*-acetylgalactosamine (3) *N*-acetylglucosamine (4) fucose, and (5) *N*-acetylneuraminic acid [22]. Lectin–carbohydrate interactions are due primarily to cooperative hydrogen-bonding wherein a hydroxyl group (OH) acts simultaneously as H-bond donor and acceptor. Water molecules may also mediate H-bonding between sugar and proteins. Polar groups of both protein amino acid residues and of sugar units also provide electrostatic stabilization while non-polar patches of sugars formed by aliphatic protons and carbons stack with tryptophan and phenylalanine residues of lectins to create non-polar interactions [23].

Lectins are polyvalent and in vitro studies show that due to their polyvalency lectins have the ability to cross-link between cells resulting in cell-agglutination. Lectin polyvalency can be inhibited by the carbohydrate for which it is specific [24]. 3D structures confirm that members of each lectin group have conserved residues at the core of its carbohydrate binding site that provide H-bonding to sugars. This core is flanked by two variable loops that provide additional *van der Waals* and H-bond interactions [25]. Due to the high selectivity of lectins to specific glycan structures, lectins are now used as binding ligands of affinity matrices in purification of glycoproteins and glycopeptides and also in cell separations. To create the stationary phase, lectins are commonly covalently immobilized to the surface [26]. Due to the selectivity of lectins and improved immobilization techniques, LAC is the most useful and efficient mode of separation of glycans and glycoproteins. For example, multi-lectin affinity columns were developed using different lectins for comprehensive capture of serum glycoproteins [27,28].

The current approach in glycomics is the development of more sensitive, efficient, and faster methods of glycan separation and analysis. One specific strategy is the development of new materials to be used in designing separation columns and extraction media. The conventional packed columns with uniform size porous particles have been traditionally used in these chromatographic separations. A new generation of separation media called monolithic materials has become an interesting option due to their design that allows faster, more efficient and versatile separations of glycans, glycopeptides and glycoproteins [29]. Monolithic columns are usually prepared in situ fused with silica capillary tubes by co-polymerization of cross-linking and functional monomers together with porogens and initiators. Other monoliths are silica-based and prepared via sol–gel synthesis. The applications of these monoliths are exclusive depending on their morphology and structure. They also have respective disadvantages; for example, organic polymer-based monoliths swell in organic solvents whereas silica-based monoliths are limited by their effective pH ranges. Therefore, rather than choosing the material to use in designing chromatographic separation and extraction media, it is important to optimize the nature of ligands bound to the substrate for an efficient, stable and selective capture of target analytes.

Recently, a number of efforts to modify porous polymer monoliths with gold nanoparticles (GNPs) have appeared. The GNPs are either formed in situ or by flowing a GNP dispersion through the monolith whose surface presents amine or thiol groups for binding the GNPs. Porous polymer monoliths modified with GNPs were used for the capture and separation of cysteine containing peptides [30]. These monoliths were then modified with carboxylic acid, hydroxyl, or amine terminated alkanethiols and applied to separate short peptides by capillary electrochromatography [31]. The surface chemistries were shown to be exchangeable by removal using an excess of 2-mercaptoethanol. The monoliths were also shown to separate a mixture of three proteins by nano-HPLC in either reverse phase or ion exchange mode. GNP immobilization onto amine-terminated grafted polymer chains was shown to provide a dense and homogenous coverage [32]. A polymer monolith was decorated with 20 nm gold nanoparticles onto which 3,3′-dithiodipropionic acid di(N-hydroxysuccinimide ester) (DTSP) was assembled and used to immobilize *Erythrina cristagalli* lectin (ECL) for extraction of glycoproteins with terminal galactose units on their

glycans [33]. GNP modified polymer monoliths modified with cysteine were used to separate a mixture of nucleosides in hydrophilic interaction chromatography (HILIC) mode and their modification with polyethyleneimine was used to separate a mixture of di- and tripeptides [34]. GNP decorated monoliths were found most effective for a particle size of 15, 20, or 30 nm when modified with octanethiol or octadecanethiol and used in reverse phase separation of a mixture of three proteins [35]. Strategies using photomasking have been used to create monolith columns with specific segments being GNP modified [36,37]. Application of GNP decorated polymer monoliths for mixed modes of separation by modifying the GNPs with mixture of alkanethiols, ω-mercaptoalkanoic acids, and amine-terminated alkanethiols was demonstrated for a three-protein mixture in reverse phase, cation exchange, anion exchange and mixed modes of separation [38]. GNP decorated polymer monoliths have also been applied in Au driven catalysis [39] and to create a lipase flow through reactor [40].

Nanoporous gold has been of growing interest in analytical and biosensing research due to its composition-dependent tunable porosity, sizes and morphologies. As commonly prepared by dealloying in acid or electrochemically, np-Au typically has pore dimensions in the tens of nanometers range [41]. These features make np-Au promising in electrochemical and optical detection and also in catalysis [42]. Nanoporous gold surfaces can also accommodate various chemical-surface modification and conjugation, mostly through Au-S chemistry, that can be utilized in separation methods of biomolecules [43]. One popular and simple way of fabricating np-Au is through selective dissolution (leaching or dealloying) of a gold alloy, wherein the less noble constituents are removed via oxidization when immersed in concentrated nitric acid solution [41]. The three-dimensional, interconnected nanoporous structure, as well as biocompatibility and good chemical stability make np-Au monoliths suitable for affinity separations [44].

In this work, we prepared free-standing monolithic np-Au plates referred to herein as np-Au monoliths that underwent surface chemical modifications to develop Concanavalin A (Con A)–modified np-Au monolith and showed its potential to selectively capture glycoprotein. Np-Au as a material can add to and complement the possibilities described using GNP decorated monoliths, and np-Au is relatively easy to prepare. The surface coverage of SAM and protein molecules prepared by a flow method onto the np-Au monolith was characterized using thermogravimetric analysis (TGA) and an in situ solution depletion method monitored by UV detection. The demonstrated selectivity of the developed Con A-modified np-Au monoliths to the high mannose-containing glycoprotein ovalbumin (OVA) shows its potential to be further developed as a material for chromatographic extraction of glycoproteins, which is a significant part of glycomics.

2. Materials and methods

2.1. Reagents

Ten carat yellow gold plates were purchased from Hoover and Strong, Richmond, Virginia, USA. Trace metal grade nitric acid was purchased from Fisher Scientific, Pittsburgh, Philadelphia, USA. Lyophilized powder of Concanavalin A from *Canavalia ensiformis* (Jack Bean) of ≥95.0% purity, albumin from chicken egg white (ovalbumin) of ≥98% purity

and bovine serum albumin (BSA) of ≥98% purity. HPLC grade ethanol, tris(hydroxymethyl)aminomethane (Tris), sodium chloride (NaCl), calcium chloride dihydrate ($CaCl_2$•$2H_2O$), manganese(II) chloride tetrahydrate ($MnCl_2$•$4H_2O$), α-methyl mannopyranoside, sodium hydroxide (NaOH), glycine and HPLC grade methanol were all purchased from Sigma Aldrich, St. Louis, Missouri, USA. Pre-mixed Laemmli sample buffer, 2-mercaptoethanol, trace metal grade acetic acid, and Page Ruler Plus prestained protein ladders were all purchased from Thermo Scientific, Illinois, USA. One hundred percent ethanol was purchased from Decon Laboratories, Inc., Pennsylvania, USA. Sodium dodecyl sulfate (SDS) and Coomassie Brilliant Blue R250 were purchased from Bio-Rad Laboratories, Inc., Richmond, California, USA. Milli-Q water (18.2 MΩ.cm at 25 °C) was prepared using a Simplicity UV system from Millipore Corporation, Boston, USA. All chemicals, reagents and proteins were used as received.

2.2. Apparatus

The flow cell system consisted of a home-made Teflon flow cell, C-FLEX tubing (Masterflex, Cole-Parmer Instrument Company, Illinois, USA), peristaltic pump (Model 77390-00, Cole-Parmer Instrument Company, Illinois, USA), UV–visible spectrophotometer (Model SPD-10A, SHIMADZU Scientific Instruments, Inc., Columbia, Maryland, USA) and data logger (Model USB 1608-G, Measurement Computing, Norton, Maryland, USA). Scanning electron microscopy (SEM) and energy dispersive X-ray spectroscopy (EDS) was done using JEOL JSM-6320F field emission SEM (JEOL USA, Inc., California, USA). Surface area and pore size analysis were done using a Beckman Coulter SA-3100 Gas Adsorption Surface Area and Pore Size Analyzer (Beckman Coulter, Inc. California, USA), with stated resolution of >0.01 $m^2\ g^{-1}$. A standard BET sample holder (3cc RapiTube, model number 7215 006B, Beckman Coulter, Inc. California, USA) was used to hold the np-Au samples. Thermogravimetric analysis was done using a Q500 Thermogravimetric Analyzer (TA Instruments, Delaware, USA). UV–vis scans and absorbance readings were done using a Varian Cary 50 UV–vis spectrometer (Varian Australia Pty Ltd., Victoria, Australia) and Suprasil quartz spectrophotometer cuvette with ten millimeter light path and volume capacity of three milliliters (model number 14-385-902C, Fischer Scientific, Pittsburgh, Pennsylvania, USA). Mini-PROTEAN pre-casted 4–20% polyacrylamide gel was used for SDS-PAGE in a Mini-PROTEAN Tetra Cell (Bio-Rad Laboratories, Inc., Richmond, California, USA).

2.3. Preparation and characterization of np-Au monoliths

Commercially available ten carat yellow gold plates (41.7% Au, 20.3% Ag, and 38.0% Cu) were cut into the desired dimensions – 6.0 mm × 6.0 mm × 0.25 mm for thermogravimetric characterization, 8.0 mm × 8.0 mm × 0.50 mm for solution depletion with UV detection experiments and 2.0 mm × 2.0 mm × 0.25 mm and 4.0 mm × 4.0 mm × 0.50 mm for BET surface area analysis. The cut pieces were then dealloyed by placing them in a concentrated nitric acid bath for 48 h and replenishing the acid solution after 24 h. Dealloyed monoliths were then rinsed thoroughly with Milli-Q water to neutral pH followed by rinsing with ethanol. Nanoporous gold monoliths were kept inside a vacuum desiccator until used. The exterior nanostructure of np-Au monoliths was characterized using SEM [45]. The np-Au monolith was also broken into smaller pieces and the side of a cleaved fragment was imaged

using SEM to characterize the interior nanostructure and confirm its nanoporosity. The elemental analysis was done using energy dispersive X-ray spectroscopy (EDS) at 15 kV. The specific surface area (S_{BET}) was determined using the Brunauer–Emmett–Teller (BET) method [46]. The pore volume versus diameter distribution was calculated by analyzing the adsorption branch of the isotherm using the Barrett-Joyner–Halenda (BJH) method [46].

2.4. Preparation of Con A-modified np-Au monoliths

The np-Au monolith was placed inside the Teflon flow cell, held in place using spacers, closed-tight and sealed (see supplementary information file Fig. A.1). These spacers are in the form of open Teflon frames so that the solution can flow readily through the spacer and into the next monolith. The flow cell was connected to a peristaltic pump by C-FLEX tubing, which was designed by the manufacturer to have very low protein binding, as well as good biocompatibility. A series of different LA solutions in ethanol, DMTMM in Milli-Q water, and Con A in buffer (10 mM Tris, 0.10 M NaCl, 1 mM $CaCl_2$, 1 mM $MnCl_2$ adjusted to pH 7.4) were circulated in order to modify the np-Au monolith surface at a constant rate of 0.5 mL min^{-1} with washings by their respective solvents prior and after circulation of each.

2.5. Thermogravimetric analysis

Modified np-Au monoliths were air-dried then placed in a platinum weighing pan and heated inside the thermogravimetric analyzer from room temperature to 600 °C at a ramping rate of 20 °C min^{-1}. The carrier gas used was nitrogen, which was held at a flow rate of 40 mL min^{-1}. Prior to initiating the temperature ramp, N_2 gas was allowed to flow through the sample for 5–10 min. Initial mass, mass losses and weight change percent were obtained from the analysis. Surface coverage of the molecules on np-Au monolith surface was calculated based on the net mass loss that was normalized to BET surface areas. Powdered samples were also analyzed with TGA using the same condition but up to 1050 °C. Ash residues left in the pan after pyrolysis of proteins were sent to Atlantic Microlab, Inc. (Norcross, Georgia, USA) for CHN analysis.

2.6. Characterization of loading and elution using UV detection

In order to characterize the loading of molecules onto np-Au monolith surfaces, a UV detector-data logger system was placed before the flow cell to measure the absorbance of the circulating solution before it reached the np-Au monolith and also during circulation. The circulation of each solution was stopped when no further change in the absorbance of the solution was detected. The estimated surface coverages of the molecules into the np-Au monoliths were calculated based on the number of molecules depleted during the circulation, which were calculated from the change in concentrations, and normalized to the surface area of the np-Au monolith. To characterize the elution of captured OVA, the UV detector-data logger system was connected to the flow cell containing the prepared Con A-modified np-Au monoliths. A series of solutions: buffer, 2 mL of 1 μM OVA, buffer, 2 mL of 0.1 M α-methyl mannopyranoside (AMMP), and buffer were passed through the flow cell while the A_{280} was recorded at 1 Hz.

2.7. Extraction of OVA using Con A-modified np-Au characterized by SDS-PAGE

A batch of eight Con A-modified np-Au monoliths was prepared. At the end of each 30 min cycle of circulation of 5 μM OVA and 15 μM BSA mixture, an aliquot was taken and kept. Two monoliths were initially used and after each cycle, the number of substrates was increased by adding two more monoliths. The aliquots of protein mixture were analyzed through SDS-PAGE using 4–20% polyacrylamide gel and stained using Coomassie blue. The gels were scanned using a desktop scanner.

2.8. Data analysis

All data calculations and graphing were done using Sigma Plot 12.0. Analysis of protein gel band sizes and intensities was done using ImageJ (imagej.nih.gov/ij/). Calculation of area under the curve (AUC) was done using GraphPad Prism 6.07.

3. Results and discussion

The significance of gold nanoparticles, gold films, gold nanostructure and nanoporous gold in various applications such as affinity biosensors, biocatalysis, and affinity separations is due to their frequently reported use as substrates for self-assembled monolayer (SAMs) formation [47–50]. SAM formation is a method of functionalization of the substrate wherein the surface is modified in order to present functional groups, which are supported by well-defined and organized organic assemblies. Thiols and disulfides are widely used to functionalize gold surfaces [51]. In one study, gold particles (3.5 μm) coated with octadecanethiol were used as stationary phase in reversed-phase separation of polyaromatic hydrocarbons [52]. In this work, we utilized lipoic acid (LA) SAMs on np-Au for immobilizing lectin Con A, and then use the Con A-modified np-Au monolith as a substrate to selectively capture glycoprotein for isolation and extraction applications.

3.1. Preparation of np-Au and Con A-modified np-Au monoliths

Our lab has previously reported the preparation of np-Au monoliths by selective dissolution of commercially available gold alloy plates in nitric acid [45], and these were then surface modified with C_{18}-SH [46]. Scanning electron microscope (SEM) images of the dealloyed 8 mm × 8 mm × 0.5 mm np-Au monoliths revealed interconnected ligaments and pores both in the exterior and interior of the monolith (Fig. 1a). Pore size distribution using Barrett–Joyner–Halenda (BJH) analysis of the adsorption branch resulted in a pore diameter range of predominantly 80–120 nm (Fig. 1b) and thus the material would be considered as macroporous by the IUPAC definition (> 50 nm). Through analysis using the Brunauer–Emmett–Teller (BET) method, the specific surface area of the monoliths was determined to be 6.9 ± 0.5 $m^2\ g^{-1}$ (n = 3). Dealloying of the alloy plate with a calculated geometric surface area of 1.44×10^{-4} m^2, increased the surface area by 8,403X producing a np-Au monolith with a mass of 175 mg and a surface area of 1.21 m^2. Elemental analysis of the np-Au monolith using EDS showed a composition of almost 99% gold after the dealloying process (Fig. 1c). Characterization of cleaved np-Au monoliths modified with proteins via flow method using tapping mode atomic force microscopy (AFM) revealed immobilization of significant amount of proteins in the interior of the monolith [45]. The average pore size of these np-Au monoliths was controllable by thermal annealing, i.e., the porosity of all free

standing np-Au structures decreases as the heat treatment temperature increases [46]. Our lab has also developed an electrochemical method of annealing np-Au by potential cycling [53].

The preparation of Con A-modified np-Au monoliths was done under flow condition, wherein solutions of desired molecules were circulated through the flow cell containing np-Au monoliths (Fig. 1d). Surface modification started with the formation of α-lipoic acid (LA) SAM in order to functionalize the np-Au monolith surface with carboxylic acid functional groups. The procedure of SAM formation of LA to functionalize gold surfaces has already been established [54,55]. To facilitate immobilization of lectin Con A, we further activated the carboxylic acid groups of LA via their esterification with 4-(4,6-dimethoxy-1,3,5-triazin-2-yl)-4-methylmorpholinium chloride (DMTMM). DMTMM is a water-soluble coupling reagent for activating carboxylic acids for reaction with amines to form amide bonds [56,57]. Con A molecules were immobilized through the replacement of the activated esters on np-Au monolith surface via amide bond formation. Con A is a C-type lectin from *Canavalia ensiformis* (Jack bean) seeds that belongs to a general group of lectins which requires Ca^{2+} and/or Mn^{2+} ions for full activation that binds to α-mannose and α-glucose sugar units of glycans of glycoproteins [58]. Specifically, Con A has been reported to bind to high-mannose [59] and trimannoside cores of complex type N-linked glycans [60]. Con A exists as a homotetramer in solution at pH 7.0 and as a dimer at pH 5.0 [61]; each subunit is a single polypeptide chain of 231 amino acids with molecular weight of 25.5 kDa [62].

A main advantage that we want to showcase in this study is the straightforward and reproducible preparation of the np-Au monoliths introduced here as a new material in chromatographic extraction of glycoproteins. The simple one-step preparation of np-Au monolith via selective dealloying in nitric acid overcomes the multi-step preparation of the reported AuNP-modified monolithic materials to achieve greater surface area [31,63,64]. The rigidity of the np-Au as a material in bioaffinity separations may resolve the issues of swelling in organic solvents of organic polymer materials [65]. The chemical stability of np-Au monolith and its applicability in a wide range of buffers can complement the limitation of silica based materials at high pH [66]. Moreover, the high melting point of np-Au monolith could be promising in beneficial high temperature separation of intact proteins [67]. Preparation of a np-Au monolith with a bimodal pore size distribution has been reported, and such a structure could provide large pores for high permeability and smaller pores to create a higher surface area [68]. Given that thermal annealing was able to increase the pore size and tune the morphology of the np-Au monolithic plate structure described herein [46], an np-Au material with highly permeable structure and high loading capacity similar to the reported monolithic columns [69] used in chromatographic analysis and separations could potentially be achieved.

3.2. Determination of surface coverage of LA and Con A molecules on np-Au monoliths using thermogravimetric analysis

In the present study, we used thermogravimetric analysis (TGA) to characterize the loading of molecules onto the np-Au monoliths. TGA is a destructive analytical method, which

allows for quantitative measurement of the change or rate of change in the weight of a material as a function of temperature or time. In another study, TGA has been used to quantify the loading of dodecanethiol monolayers formed on gold nanoparticles [70]. TGA has also been used to determine the temperature stability of the octadecylamine (ODA) monolayer coating gold nanoparticles [71]. Our lab has previously reported the use of TGA to analyze the one-step decomposition of octadecanethiol on np-Au [46]. We further used TGA in assessing the loading of biomolecules, enabling us to demonstrate lectin–carbohydrate interactions on np-Au monoliths [72]. In the current study, we quantified the amount of molecules loaded onto the np-Au monolith using TGA allowing us to determine the surface coverage of the molecules being immobilized taking into account the specific surface area of the np-Au. We subjected the air-dried modified np-Au monoliths to pyrolitic decomposition in an inert environment while scanning up to 600 °C. At this temperature, both LA and DMTMM molecules were expected to be completely decomposed. Pyrolysis of the LA and DMTMM powders resulted in complete decomposition before the temperature reached 600 °C (see supplementary information file, Fig. A.2). In contrast, proteins were not completely decomposed and left some solid ash residue on the pan after scanning up to 1050 °C (see supplementary information file, Fig. A.2). CHN analysis of the residue resulted in 70% C, 2.5% H, 11.8% N with a C:H:N ratio of 35:1:5.5. The result was little changed by holding the temperature at 600 °C for two hours, with the CHN analysis then being 69% C, 2.6% H, and 11.0% N. The lyophilized powder of the protein has a theoretical composition of 46% C, 8% H and 14% N by mass with C:H:N of 5.75:1:1.75. Clearly, the residue after the pyrolysis was mostly composed of carbon. Having these results, the mass losses due to proteins were multiplied by factors of 1.20 to determine the total protein mass being loaded into np-Au monolith. TGA was capable of resolving mass losses to 0.1 μg and therefore suited to report loading of micrograms of molecules onto a single np-Au monolith.

The np-Au monolith modified by 1 h of circulation of a 1 mM LA solution in ethanol and referred to here as “SAM-modified np-Au monolith” was subjected to TGA and found to lose 0.30% of its mass during the temperature scan (Fig. 2a). This mass loss corresponded to 0.4485 mg m^{-2} of LA self-assembled onto the np-Au monolith surface giving a corresponding surface coverage of 1.31×10^{18} molecules m^{-2}. Based on theoretical estimates, a complete and ordered coverage of LA molecules on a gold surface would have resulted in $3.45 \times 10^{18} – 4.40 \times 10^{18}$ molecules m^{-2}. This range was calculated based on the three possible surface areas (0.91 nm^2, 1.09 nm^2, and 1.16 nm^2) using the reported crystal structure unit cell dimensions of LA: a = 11.744 Å, b = 9.895 Å, c = 9.246 Å, where there were four LA molecules per unit cell [73]. This suggests that the LA molecules assembled in a disorderedly fashion on np-Au monolith surface with possible incompleteness of coverage. Reported surface coverages of LA on flat gold surfaces are 3.00×10^{-10} mol cm^{-2} (1.81×10^{18} molecules m^{-2}) [74], 3.50×10^{-10} mol cm^{-2} (2.11×10^{18} molecules m^{-2}) [75] and 2.42×10^{-10} mol cm^{-2} (1.46×10^{18} molecules m^{-2}) [76]. An additional TGA mass loss of 0.1311 mg m^{-2}. np-Au was found during the temperature scan of SAM-modified np-Au subjected to DMTMM activation of carboxylic acids to esters and increased the weight change percent to 0.39% (Fig. 2a). We tested the stability of the SAM formed on the np-Au monolith by washing it with binding buffer for another 7 h; the TGA mass loss was 0.41%

which was an insignificant change when compared to that for the one washed for only 30 min (0.39%) (Fig. 2a).

The SAM-modified and activated np-Au monolith was further modified by 3 h circulation of a 10 μM Con A solution in buffer and referred to here as "Con A-modified np-Au monolith" was also subjected to TGA and found to lose 0.47% of its mass corresponding to an additional 0.3135 mg m^{-2} during the temperature scan (Fig. 2b). This mass loss was calculated by subtracting the mass loss of the SAM-modified np-Au monolith from the mass loss found for the Con A-modified np-Au monolith and then multiplying by the factor of 1.2. Therefore, only the mass of Con A molecules being immobilized was accounted for and this resulted in a surface coverage of 1.85×10^{15} molecules m^{-2}. The maximum possible surface coverage for Con A is estimated as 1.29×10^{16}–1.82×10^{16} molecules m^{-2} based on the unit cell dimensions of tetrameric Con A (PDB ID: 3CNA) a = 63.15 Å, b = 86.91 Å, c = 89.25 Å [62] and assuming three possible surface areas per molecule of 54.8 nm^2, 56.4 nm^2 and 77.6 nm^2 calculated assuming that the Con A molecules lay flat and that they pack side-by side. The surface coverage of LA and Con A molecules obtained by TGA suggests partial but extensive surface coverage of Con A molecules on SAM-modified np-Au monoliths. We also tested the stability of immobilized Con A molecules by additional washing with buffer for another 3 h after the immobilization. An insignificant change in mass loss (0.46%) was seen after longer washing of 4 h when compared to the Con A-modified np-Au monolith washed for only 30 min (0.47%) (Fig. 2b). The observed insignificant mass loss suggests that the covalently immobilized Con A remained bound to the surface for at least another 3 h under flow conditions.

3.3. In situ solution depletion method using UV detection in determining surface coverage of molecules on np-Au monolith

We further developed a method wherein the modification of the np-Au monolith surface can be characterized in situ. Using this non-destructive method, the substrate could possibly be regenerated. A UV detector-data logger system was used to observe the change in absorbance of the circulating solution due to the loss of molecules from the solution while being loaded onto the np-Au monolith. We initially constructed calibration curves for LA and Con A solution by plotting the different analytical concentrations of the solution versus the corresponding UV detector-data logger system readings. Good linear correlations were observed for both analytes and the factors 0.0502 mM^{-1} for LA (see supplementary information file, Fig. A.3a) and 0.0329 μM^{-1} for Con A (see supplementary information file, Fig. A.3b) were obtained from the slopes of the linear regressions. These factors were then used to convert the UV detector-data logger system readings to the corresponding concentration in the analysis of the loading curves. Circulating LA solution in ethanol was observed at wavelength (λ_{max}) of 330 nm, which was obtained from the UV scan (Fig. 3a). The absorption band of LA molecules in solution is due to the strained five-membered cyclic disulfide structure [77]. On the other hand, the circulating protein solutions in buffer were observed at λ_{max} = 280 nm (Fig. 3b); the absorbance was due to the tryptophan (Trp) and tyrosine (Tyr) residues and to the disulphide bonds formed between cysteine residues of the peptides to form cystine residues (Cys). Tetrameric Con A has 16 tryptophan (Trp) and 28 tryrosine (Tyr) residues [78]. The glycoprotein OVA, on the other hand, contains 3 Trp,

10 Try and 1 Cys residues [79] and the non-glycoprotein BSA has 2 Trp, 20 Tyr and 17 Cys residues [79]. The ε_{330} of the LA solution was experimentally determined to be 0.1617 mM^{-1} cm^{-1} (see supplementary information file Fig. A.4). This value was the slope of the linear regression fit to the plot of different analytical concentrations versus A_{330} using the UV-vis spectrophotometer. The ε_{280} values of proteins were calculated as the weighted sum of the ε_{280} values of Trp, Tyr and Cys using the proposed equation: ε_{280} (M^{-1} cm^{-1}) = no. of Tryptophan × 5,500 + no. of Tyrosine × 1,490 + no. of Cystines × 125 [79]. The values were as follows: ε_{280}(Con A) = 129,720 M^{-1} cm^{-1}, ε_{280}(OVA) = 31, 525 M^{-1} cm^{-1} [79], and ε_{280}(BSA) = 42,925M^{-1} cm^{-1} [79]. These extinction coefficients were used in the preparation of the LA and Con A solutions during the study.

Circulation of 3 mL of 1 mM LA solution through 175 mg np-Au monolith resulted in a change of concentration of 0.663 mM; this corresponded to 1.20×10^{18} LA molecules lost from the 3 mL solution (Fig. 3c). Normalizing this amount of molecules to the calculated 1.21 m^2 surface area of the np-Au monolith resulted in a surface coverage of 0.989×10^{18} molecules m^{-2}. The volume of the circulating solution was based on the surface coverage estimated by TGA, assuring that there were enough molecules available in the solution for the np-Au monolith being used. For example, a 175 mg np-Au monolith with surface area of 1.21 m^2 would have contained 1.66×10^{18} LA molecules on the basis of 1.37×10^{18} molecules m^{-2} surface coverage. The 3 mL solution of 1 mM LA contains 1.81×10^{18} LA molecules. Circulation of 3 mL of 6 μM Con A solution on SAM-modified np-Au monolith resulted in a change in concentration of 0.891 μM (Fig. 3d). This corresponded to 1.61×10^{15} Con A molecules lost from a 3 mL solution. Normalizing to 1.21 m^2 resulted in coverage of 1.32×10^{15} molecules m^{-2}. Likewise, 3 mL of 6 μM Con A solution contained 1.08×10^{16} Con A molecules and was sufficient based on the amount of Con A molecules (2.24×10^{15}) using the surface coverage of Con A molecules characterized by TGA. The concentration of 10 μM used in TGA was decreased to 6 μM in this method so the A_{280} readings would not exceed 1.0 and diluted enough to obey the linearity of absorbance with concentration according to the Beer–Lambert Law. The method using the UV detector was developed to provide a procedure that can determine when to stop the circulation with the assurance that there were no longer available sites on the surface of np-Au available for the immobilization of molecules. This method could be also used to further study and to determine binding kinetic parameters. The surface coverages found by the thermogravimetric analysis approach are generally larger both for LA and for Con A. TGA quantifies the molecules on the np-Au monolith after washing steps and drying. The solution depletion method, on the other hand, quantifies the molecules by a two-point absorbance difference for a continuously flowing solution. It is possible that additional molecules that are not bound to the surface become trapped inside the monolith when it is removed and subjected to TGA. The possible positive baseline drift of UV detection method could also be responsible for the lower estimation of surface coverage found using this method [80].

3.4. Characterization of selective capture of OVA using Con A-modified np-Au monoliths

Our chosen model glycoprotein is chicken egg white ovalbumin (OVA) with a molecular weight of 44.3 kDa. OVA is glycosylated mainly with high-mannose and hybrid structures [81], therefore it binds to Con A with high specificity. We used bovine serum albumin

(BSA), a 66.4 kDa non-glycosylated protein, as a negative control. The three estimated areas per molecule occupied by OVA provided that we assume adsorption of the solid state conformation on the surface oriented on a face of the unit cell are 45 nm^2, 53 nm^2 and 61 nm^2 based on the reported unit cell dimensions (PDB ID: 1OVA) a = 53.27 Å, b = 44.97 Å, c = 60.56 Å [82]. On the other hand, there are four BSA molecules per unit cell with reported unit cell dimensions (PDB ID: 4F5S) of a = 217.80 Å, b = 44.99 Å, c = 143.06 Å [83]. The possible footprints of OVA and BSA molecules adsorbed onto modified np-Au surfaces will be affected by the conformational changes the proteins undergo in solution. Changes in proteins structure in solution are dependent on pH, ionic strength and temperature [84,85]. For example, in solution below pH 4, BSA has been described as a prolate ellipsoid (E-form) with dimensions of 4.0 nm × 4.0 nm × 14.0 nm; however, it adopts the N-form of dimensions 3.0 nm × 8.0 nm × 8.0 nm between pH 4.5 – 8.0 [86] and therefore in our experiments it is most likely the N-form that becomes surface bound. BSA dimensions on the surface are therefore likely to be those of the N-form however the orientation is not certain. The footprint of BSA on the surface could be estimated to range from as low as 24 nm^2 to as much as 64 nm^2. BSA is monomeric in solution but OVA has been reported to form dimers with a radius of gyration of 2.7 nm [87]. Moreover, proteins undergo conformational changes upon adsorption on solid surfaces [88,89]. These uncertainties in protein sizes in solution make it difficult to assign a size factor based on a clearly known difference in area occupied per adsorbed protein molecule; however, it appears plausible that the areas occupied by each of these proteins on the surface do not differ by more than a factor of two and could be closer.

We circulated 10 μM OVA solution in buffer for 1 h through a Con A-modified np-Au monolith. A mass loss of 0.64% accounted for an additional mass of 0.3098 mg m^{-2} to the mass loss from Con A-modified np-Au monolith due to the captured OVA molecules. This resulted in a surface coverage of 4.21×10^{15} OVA molecules m^{-2} (Fig. 4a) and OVA:Con A ratio of 2.3. On the other hand, circulation of the 10 μM BSA solution for 1 h through the Con A-modified np-Au resulted in an additional mass loss of 0.2899 mg m^{-2} and a weight change of 0.63% that corresponded to a surface coverage of 2.63×10^{15} BSA molecules m^{-2} on np-Au and BSA:Con A ratio of 1.4 (Fig. 4a). The greater surface coverage of OVA than BSA to Con A-modified np-Au monolith suggests some selectivity of the substrate for the OVA molecules. The high BSA:Con A ratio and the partial coverage of Con A to the SAM-modified np-Au monolith led us to suspect that there could be some non-specific adsorption of BSA molecules onto the “unused” activated esters still available for protein immobilization. To minimize this non-specific adsorption caused by “free” activated esters, we circulated a 1% (v/v) ethanolamine solution prior to the capture of OVA or BSA to “cap” the “unused” reactive esters and convert them to hydroxyls that were not capable of covalently immobilizing proteins. We initially tested the effectivity of the capping procedure by circulating ethanolamine solution over the activated SAM prior to Con A circulation. TGA showed an insignificant amount of Con A added to the mass loss of SAM-modified np-Au monolith capped and suggests that immobilization by non-specific adsorption was restricted (Fig. 4b). Employing the capping procedure to the Con A modified monolith prior to the capture of OVA gave a weight change of 0.59% or a surface coverage of 3.51×10^{15} molecules m^{-2} np-Au and OVA:Con A ratio of 2.19. The capping procedure allowed only a

weight change of 0.48% for BSA or a surface coverage of 0.533×10^{15} molecules m^{-2} np-Au and BSA:Con A ratio of 0.33 (Fig. 4c). Therefore, the capping procedure enhanced selectivity by greatly reducing the non-specific adsorption of BSA. The disordered structure of the lipoic acid SAMs and their likely incomplete coverage of the Au surface may allow for a degree of non-specific adsorption onto the np-Au monolith, and thus optimization of the SAM structure and coverage could be a strategy for improving the selectivity. A possible strategy for improving the selectivity would be to introduce a spacer chain onto the LA based on oligo (ethylene glycol) that is terminated in a carboxylic acid group, as such a LA derivative would better resist non-specific protein adsorption to regions of the SAM that are between immobilized Con A proteins.

3.5. Extraction of OVA from a mixture using Con A-modified np-Au monolith

To demonstrate the application of Con A-modified np-Au monolith in extracting and isolating OVA from a mixture, we prepared a mixture of 5 μM OVA and 15 μM BSA, circulated it through the Con A-modified np-Au monoliths and observed how the concentrations of these proteins depleted over time. We initially prepared a batch of Con A-modified np-Au monoliths. The 1:3 OVA:BSA mixtures were circulated for 30 min per cycle, and at the start of each cycle a new set of Con A-modified np-Au monoliths were added and an aliquot of the circulating solution was obtained at the end of each cycle and kept (Fig. 5a). OVA and BSA, having molar masses of 66.4 kDa and 44.3 kDa, respectively, appeared at different positions on 4–20% polyacrylamide gel run through SDS-PAGE and stained by Coomassie blue (Fig. 5b). The size and intensity of protein bands in the gel were analyzed using ImageJ (Fig. 5b). The size and intensity of the band of BSA aliquot 4 (after the cycles) was 74.58% of aliquot 0 (before the cycles). The initial 2 mL 15 μM BSA solution contained 1.81×10^{16} molecules. Therefore, after the cycles, it could be estimated that 1.35×10^{16} BSA molecules were remaining in the solution and that 4.56×10^{15} molecules have been depleted. On the other hand, the size and intensity of the band of OVA aliquot 4 was 11.74% of the initial solution.The initial 2 mL of 5 μM OVA solution contained 6.02×10^{15} molecules. There were thus approximately 0.707×10^{15} molecules left in the solution and 5.31×10^{15} molecules were depleted. Thus, the Con A-modified np-Au monoliths were able to capture a significant amount of OVA molecules in the presence of an excess of BSA. The captured BSA molecules could be washed off after the cycles, and so the captured OVA could be isolated. This demonstrated the affinity of the Con A-modified np-Au monoliths for OVA, and thus these glycoproteins can be extracted from a mixture using the developed substrates.

3.6. Elution of captured OVA

The captured OVA molecules by Con A-modified np-Au monoliths were eluted using a solution of a high concentration of ligand α-methyl mannopyranoside in buffer. Lectin–carbohydrate interactions are reversible and therefore the binding would be able to be undone by a competitive ligand. We established a chromatogram using a UV detector by recording the A_{280} at 1 Hz. Flowing 1 μM OVA into the flow cell without the Con A-modified np-Au monolith established a peak with AUC of 1.898 ± 0.073 (n = 3) (Fig. 6a). This represented the amount of OVA molecules in a 2 mL 1 μM solution, which was 1.20×10^{15} molecules. When this solution flowed through the developed substrate, the AUC

decreased to 1.330 (Fig. 6b). The difference of 0.568 represented the amount of OVA (approximately 0.36×10^{15} molecules) being captured by the Con A-modified monolith. When free ligand AMMP solution was flowed through the substrate after the washing, a peak was established with AUC of 0.4696 (Fig. 6b). This represented the amount of OVA being eluted. The eluted amount was 83% of the amount of captured OVA.

4. Conclusion

In this work, np-Au monolith surface modified with affinity ligands Con A were developed to create a stationary phase used in chromatographic separation and extraction of intact glycoproteins. Np-Au can be prepared by a fairly straightforward acid dealloying step followed by proceeding directly to surface modification. The capture of target glycoproteins in the mobile phase was due to the reversible affinity of the carbohydrate residues of glycoproteins to the carbohydrate-binding domain of the immobilized lectins. TGA and a UV-detected in situ solution depletion method were used to determine the surface coverage of LA molecules forming SAMs. These SAMs were further utilized in covalent immobilization of Con A molecules that were found to have partial surface coverage. The function of the immobilized Con A was preserved as shown by the demonstrated selectivity of the substrate to high mannose-containing OVA versus non-glycosylated BSA. The selectivity was enhanced by reducing non-specific adsorption of proteins to the unutilized activated functional esters on the surface after Con A immobilization by using a capping reaction. The high surface area-to-volume ratio, robustness, chemical stability and biocompatibility of np-Au monoliths in addition to the wide range of available surface modification are the potential advantages of this developed lectin-modified np-Au monoliths for separation of intact glycoproteins and glycopeptides. The results of this work can be used as framework for further developments that may focus on optimizing monolayer structure to limit non-specific adsorption, tuning of experimental parameters, and use of other lectins and possibly other ligands in chromatographic separations of biomolecules by a variety of interaction modes.

Supplementary Material

Refer to Web version on PubMed Central for supplementary material.

Acknowledgments

The authors thank Dr. David Osborn for helpful discussions concerning the BET, TGA, and SEM instrumentation located in the UM-St. Louis Center for Nanoscience and Dr. Michael R. Nichols laboratory for guidance on SDS-PAGE. This work was supported by UM-St. Louis and by the NIGMS award R01-GM090254.

References

1. Varki A. Biological roles of oligosaccharides: All of the theories are correct. Glycobiology. 1993; 3:97–130. [PubMed: 8490246]
2. Brandley BK, Schnaar RL. Cell-surface carbohydrates in cell recognition and response. J Leukoc Biol. 1986; 40:97–111. [PubMed: 3011937]
3. Helenius A, Aebi M. Intracellular functions of N-linked glycans. Science. 2001; 291:2364–9. [PubMed: 11269317]

4. Mechref Y, Hu Y, Garcia A, Hussein A. Identifying cancer biomarkers by mass spectrometry-based glycomics. Electrophoresis. 2012; 33:1755–67. [PubMed: 22740464]
5. Wanebo HJ, Rao B, Pinsky CM, Hoffman RG, Stearns M, Schwartz MK, Oettgen HF. Preoperative carcinoembryonic antigen level as a prognostic indicator in colorectal cancer. N Engl J Med. 1978; 299:448–51. [PubMed: 683276]
6. Thompson IM, Pauler DK, Goodman PJ, Tangen CM, Lucia MS, Parnes HL, Minasian LM, Ford LG, Lippman SM, Crawford ED, Crowley JJ, Coltman CA. Prevalence of prostate cancer among men with a prostate-specific antigen level ≤4.0 ng per milliliter. N Engl J Med. 2004; 350:2239–2246. [PubMed: 15163773]
7. Cummings RD, Pierce JM. The challenge and promise of glycomics. Chem Biol. 2014; 21:1–15. [PubMed: 24439204]
8. Zaia J. Mass spectrometry and the emerging field of glycomics. Chem Biol. 2008; 15:881–92. [PubMed: 18804025]
9. Mechref Y, Novotny MV. Structural investigations of glycoconjugates at high sensitivity. Chem Rev. 2002; 102:321–69. [PubMed: 11841246]
10. Wuhrer M. Glycomics using mass spectrometry. Glycoconj J. 2013; 30:11–22. [PubMed: 22532006]
11. Duus J, Gotfredsen CH, Bock K. Carbohydrate structural determination by NMR spectroscopy: Modern methods and limitations. Chem Rev. 2000; 100:4589–614. [PubMed: 11749359]
12. Bertók T, Katrlík J, Gemeiner P, Tkac J. Electrochemical lectin based biosensors as a label-free tool in glycomics. Microchim Acta. 2013; 180:1–13.
13. Liu Y, Shu C, Lamb JD. High-performance capillary electrophoretic separation of carbohydrates with indirect UV detection using diethylamine and borate as electrolyte additives. J Capillary Electrophor. 1997; 4:97–103. [PubMed: 9484655]
14. Sawa M, Hsu T, Itoh T, Sugiyama M, Hanson SR, Vogt PK, Wong C. Glycoproteomic probes for fluorescent imaging of fucosylated glycans in vivo. Proc Nat Acad of Sci U S A. 2006; 103:12371–12376.
15. Kuno A, Uchiyama N, Koseki-Kuno S, Ebe Y, Takashima S, Yamada M, Hirabayashi J. Evanescent-field fluorescence-assisted lectin microarray: a new strategy for glycan profiling. Nat Methods. 2005; 2:851–6. [PubMed: 16278656]
16. Chen S, Haab BB. Analysis of glycans on serum proteins using antibody microarrays. Methods Mol Biol. 2009; 520:39–58. [PubMed: 19381946]
17. Kuster B, Wheeler SF, Hunter AP, Dwek RA, Harvey DJ. Sequencing of N-linked oligosaccharides directly from protein gels: in-gel deglycosylation followed by matrix-assisted laser desorption/ionization mass spectrometry and normal-phase high-performance liquid chromatography. Anal Biochem. 1997; 250:82–101. [PubMed: 9234902]
18. Mechref Y. Analysis of glycans derived from glycoconjugates by capillary electrophoresis-mass spectrometry. Electrophoresis. 2011; 32:3467–81. [PubMed: 22180203]
19. Wuhrer M, Deelder AM, Hokke CH. Protein glycosylation analysis by liquid chromatography-mass spectrometry. J Chromatogr B Analyt Technol Biomed Life Sci. 2005; 825:124–33.
20. Que AH, Novotny MV. Structural characterization of neutral oligosaccharide mixtures through a combination of capillary electrochromatography and ion trap tandem mass spectrometry. Anal Bioanal Chem. 2003; 375:599–608. [PubMed: 12638042]
21. Derewenda Z, Yariv J, Helliwell JR, Kalb AJ, Dodson EJ, Papiz MZ, Wan T, Campbell J. The structure of the saccharide-binding site of Concanavalin A. EMBO J. 1989; 8:2189–2193. [PubMed: 2792084]
22. Lis H, Sharon N. Lectins: Carbohydrate-specific proteins that mediate cellular recognition. Chem Rev. 1998; 98:637–674. [PubMed: 11848911]
23. Weis WI, Drickamer K. Structural basis of lectin-carbohydrate recognition. Annu Rev Biochem. 1996; 65:441–73. [PubMed: 8811186]
24. Sharon N, Lis H. Lectins: cell-agglutinating and sugar-specific proteins. Science. 1972; 177:949–59. [PubMed: 5055944]
25. Loris R. Principles of structures of animal and plant lectins. Biochim Biophys Acta. 2002; 1572:198–208. [PubMed: 12223270]

26. Bedair M, Oleschuk RD. Lectin affinity chromatography using porous polymer monolith assisted nanoelectrospray MS/MS. Analyst. 2006; 131:1316–21. [PubMed: 17124539]
27. Yang Z, Hancock WS. Approach to the comprehensive analysis of glycoproteins isolated from human serum using a multi-lectin affinity column. J Chromatogr A. 2004; 1053:79–88. [PubMed: 15543974]
28. Selvaraju S, El Rassi Z. Tandem lectin affinity chromatography monolithic columns with surface immobilised Concanavalin A, wheat germ agglutinin and Ricinus communis agglutinin-I for capturing sub-glycoproteomics from breast cancer and disease-free human sera. J Sep Sci. 2012; 35:1785–95. [PubMed: 22807361]
29. Alla AJ, Stine KJ. Development of monolithic column materials for the separation and analysis of glycans. Chromatography. 2015; 2:20–65.
30. Xu Y, Cao Q, Svec F, Fréchet JMJ. Porous polymer monolithic column with surface-bound gold nanoparticles for the capture and separation of cysteine-containing peptides. Anal Chem. 2010; 82:3352–3358. [PubMed: 20302345]
31. Cao Q, Xu Y, Liu F, Svec F, Fréchet JMJ. Polymer monoliths with exchangeable chemistries: Use of gold nanoparticles as intermediate ligands for capillary columns with varying surface functionalities. Anal Chem. 2010; 82:7416–7421. [PubMed: 20681590]
32. Connolly D, Twamley B, Paull B. High-capacity gold nanoparticle functionalised polymer monoliths. Chem Commun. 2010; 46:2109–2111.
33. Alwael H, Connolly D, Clarke P, Thompson R, Twamley B, O'Connor B, Paull B. Pipette-tip selective extraction of glycoproteins with lectin modified gold nano-particles on a polymer monolithic phase. Analyst. 2011; 136:2619–28. [PubMed: 21552581]
34. Lv Y, Lin Z, Svec F. Hypercrosslinked large surface area porous polymer monoliths for hydrophilic interaction liquid chromatography of small molecules featuring zwitterionic functionalities attached to gold nanoparticles held in layered structure. Anal Chem. 2012; 84:8457–60. [PubMed: 22998108]
35. Lv Y, Alejandro FM, Fréchet JMJ, Svec F. Preparation of porous polymer monoliths featuring enhanced surface coverage with gold nanoparticles. J Chromatogr A. 2012; 1261:121–128. [PubMed: 22542442]
36. Guerrouache M, Mahouche-Chergui S, Chehimi MM, Carbonnier B. Site-specific immobilisation of gold nanoparticles on a porous monolith surface by using a thiol-yne click photopatterning approach. Chem Commun. 2012; 48:7486–7488.
37. Currivan S, Connolly D, Paull B. Production of polymer monolithic capillary columns with integrated gold nano-particle modified segments for on-capillary extraction. Microchem J. 2013; 111:32–39.
38. Terborg L, Masini JC, Lin M, Lipponen K, Riekolla ML, Svec F. Porous polymer monolithic columns with gold nanoparticles as an intermediate ligand for the separation of proteins in reverse phase-ion exchange mixed mode. J Adv Res. 2015; 6:441–448. [PubMed: 26257942]
39. Floris P, Twamley B, Nesterenko P, Paull B, Connolly D. Fabrication and characterisation of gold nano-particle modified polymer monoliths for flow-through catalytic reactions and their application in the reduction of hexacyanoferrate. Microchim Acta. 2014; 181:249–256.
40. Lv Y, Lin Z, Tan T, Svec F. Preparation of reusable bioreactors using reversible immobilization of enzyme on monolithic porous polymer support with attached gold nanoparticles. Biotechnol Bioeng. 2014; 111:50–58. [PubMed: 23860941]
41. Seker E, Reed M, Begley M. Nanoporous gold: Fabrication, characterization, and applications. Materials. 2009; 2:2188.
42. Ding Y, Chen M. Nanoporous metals for catalytic and optical applications. MRS Bull. 2009; 34:569–576.
43. Tan YH, Pandey B, Sharma A, Bhattarai J, Stine KJ. Bioconjugation reactions for covalent coupling of proteins to gold surfaces. Global J Biochem. 2012; 3:1–21.
44. Zheng LT, Wei YL, Gong HQ, Qian L. Application progress of nanoporous gold in analytical chemistry. Chin J Anal Chem. 2013; 41:137–144.

45. Tan YH, Schallom JR, Ganesh NV, Fujikawa K, Demchenko AV, Stine KJ. Characterization of protein immobilization on nanoporous gold using atomic force microscopy and scanning electron microscopy. Nanoscale. 2011; 3:3395–407. [PubMed: 21750834]
46. Tan YH, Davis JA, Fujikawa K, Ganesh NV, Demchenko AV, Stine KJ. Surface area and pore size characteristics of nanoporous gold subjected to thermal, mechanical, or surface modification studied using gas adsorption isotherms, cyclic voltammetry, thermogravimetric analysis, and scanning electron microscopy. J Mater Chem. 2012; 22:6733–6745. [PubMed: 22822294]
47. Chaki NK, Vijayamohanan K. Self-assembled monolayers as a tunable platform for biosensor applications. Biosens Bioelectron. 2002; 17:1–12. [PubMed: 11742729]
48. Qiu H, Li Y, Ji G, Zhou G, Huang X, Qu Y, Gao P. Immobilization of lignin peroxidase on nanoporous gold: Enzymatic properties and in situ release of H_2O_2 by co-immobilized glucose oxidase. Bioresour Technol. 2009; 100:3837–42. [PubMed: 19349165]
49. Sykora D, Kasicka V, Miksik I, Rezanka P, Zaruba K, Matejka P, Kral V. Application of gold nanoparticles in separation sciences. J Sep Sci. 2010; 33:372–87. [PubMed: 20099261]
50. Bhattarai JK, Sharma A, Fujikawa K, Demchenko AV, Stine KJ. Electrochemical synthesis of nanostructured gold film for the study of carbohydrate–lectin interactions using localized surface plasmon resonance spectroscopy. Carbohydr Res. 2015; 405:55–65. [PubMed: 25442712]
51. Love JC, Estroff LA, Kriebel JK, Nuzzo RG, Whitesides GM. Self-assembled monolayers of thiolates on metals as a form of nanotechnology. Chem Rev. 2005; 105:1103–69. [PubMed: 15826011]
52. Qu QS, Zhang XX, Zhao ZZ, Hu XY, Yan C. Gold microspheres modified with octadecanethiol for capillary liquid chromatography. J Chromatogr A. 2008; 1198–1199:95–100. [PubMed: 22422014]
53. Sharma A, Bhattarai JK, Alla AJ, Demchenko AV, Stine KJ. Electrochemical annealing of nanoporous gold by application of cyclic potential sweeps. Nanotechnology. 2015; 26:085602. [PubMed: 25649027]
54. Carofiglio T, Fornasier R, Jicsinszky L, Tonellato U, Turco C. Synthesis, characterization and chemisorption on gold of a β-cyclodextrin–lipoic acid conjugate. Tetrahedron Lett. 2001; 42:5241–5244.
55. Sharma J, Chhabra R, Andersen CS, Gothelf KV, Yan H, Liu Y. Toward reliable gold nanoparticle patterning on self-assembled DNA nanoscaffold. J Am Chem Soc. 2008; 130:7820–7821. [PubMed: 18510317]
56. Kunishima M, Kawachi C, Monta J, Terao K, Iwasaki F, Tani S. 4-(4,6-dimethoxy-1,3,5-triazin-2-yl)-4-methyl-morpholinium chloride: an efficient condensing agent leading to the formation of amides and esters. Tetrahedron. 1999; 55:13159–13170.
57. Kamiński ZJ, Paneth P, Rudziński J. A study on the activation of carboxylic acids by means of 2-chloro-4,6-dimethoxy-1,3,5-triazine and 2-chloro-4,6-diphenoxy-1,3,5-triazine. J Org Chem. 1998; 63:4248–4255.
58. Derewenda Z, Yariv J, Helliwell JR, Kalb AJ, Dodson EJ, Papiz MZ, Wan T, Campbell J. The structure of the saccharide-binding site of concanavalin A. Embo J. 1989; 8:2189–93. [PubMed: 2792084]
59. Mandal DK, Kishore N, Brewer CF. Thermodynamics of lectin-carbohydrate interactions. Titration microcalorimetry measurements of the binding of N-linked carbohydrates and ovalbumin to Concanavalin A. Biochemistry. 1994; 33:1149–1156. [PubMed: 8110746]
60. Naismith JH, Field RA. Structural basis of trimannoside recognition by Concanavalin A. J Biol Chem. 1996; 271:972–976. [PubMed: 8557713]
61. McKenzie GH, Sawyer WH. The binding properties of dimeric and tetrameric Concanavalin A: Binding of ligands to non-interacting macromolecular acceptors. J Biol Chem. 1973; 248:549–556. [PubMed: 4684692]
62. Hardman KD, Ainsworth CF. Structure of concanavalin A at 2.4-A resolution. Biochemistry. 1972; 11:4910–9. [PubMed: 4638345]
63. Xu Y, Cao Q, Svec F, Frechet JM. Porous polymer monolithic column with surface-bound gold nanoparticles for the capture and separation of cysteine-containing peptides. Anal Chem. 2010; 82:3352–8. [PubMed: 20302345]

64. Connolly D, Twamley B, Paull B. High-capacity gold nanoparticle functionalised polymer monoliths. Chem Commun. 2010; 46:2109–11.
65. Sun J, Jordan LR, Forsyth M, MacFarlane DR. Acid–organic base swollen polymer membranes. Electrochim Acta. 2001; 46:1703–1708.
66. Kirkland JJ, Henderson JW, DeStefano JJ, van Straten MA, Claessens HA. Stability of silica-based, endcapped columns with pH 7 and 11 mobile phases for reversed-phase high-performance liquid chromatography. J Chromatogr A. 1997; 762:97–112. [PubMed: 9098970]
67. Blackler AR, Speers AE, Wu CC. Chromatographic benefits of elevated temperature for the proteomic analysis of membrane proteins. Proteomics. 2008; 8:3956–3964. [PubMed: 18780350]
68. Lee MN, Santiago-Cordoba MA, Hamilton CE, Subbaiyan NK, Duque JG, Obrey KAD. Developing monolithic nanoporous gold with hierarchical bicontinuity using colloidal bijels. J Phys Chem Lett. 2014; 5:809–812. [PubMed: 26274071]
69. Guiochon G. Monolithic columns in high-performance liquid chromatography. J Chromatogr A. 2007; 1168:101–68. discussion 100. [PubMed: 17640660]
70. Gross GM, Nelson DA, Grate JW, Synovec RE. Monolayer-protected gold nanoparticles as a stationary phase for open tubular gas chromatography. Anal Chem. 2003; 75:4558–4564. [PubMed: 14632064]
71. Qu Q-S, Shen F, Shen M, Hu X-Y, Yang G-J, Wang C-Y, Yan C, Zhang Y-K. Open-tubular gas chromatography using capillary coated with octadecylamine-capped gold nanoparticles. Anal Chim Acta. 2008; 609:76–81. [PubMed: 18243876]
72. Tan YH, Fujikawa K, Pornsuriyasak P, Alla AJ, Ganesh NV, Demchenko AV, Stine KJ. Lectin-carbohydrate interactions on nanoporous gold monoliths. New J Chem. 2013; 37:2150–2165.
73. Stroud, RMaC; CH. A single-crystal structure determination of DL-6-thioctic acid, $C_8H_{14}O_2S_2$. Acta Cryst. 1972; B28:304–307.
74. Wang Y, Kaifer AE. Interfacial molecular recognition. Binding of ferrocenecarboxylate to β-Aminocyclodextrin hosts electrostatically immobilized on a thioctic acid monolayer. J Phys Chem B. 1998; 102:9922–9927.
75. Madoz J, Kuznetzov BA, Medrano FJ, Garcia JL, Fernandez VM. Functionalization of gold surfaces for specific and reversible attachment of a fused β-galactosidase and choline-receptor protein. J Am Chem Soc. 1997; 119:1043–1051.
76. Pandey B, Demchenko AV, Stine KJ. Nanoporous gold as a solid support for protein immobilization and development of an electrochemical immunoassay for prostate specific antigen and carcinoembryonic antigen. Microchim Acta. 2012; 179:71–81.
77. Matsugo S, Han D, Tritschler HJ, Packer L. Decomposition of alpha-lipoic acid derivatives by photoirradiation-formation of dihydrolipoic acid from alpha-lipoic acid. Biochem Mol Biol Int. 1996; 38:51–9. [PubMed: 8932519]
78. Agrawal BB, Goldstein IJ. Protein-carbohydrate interaction. VII. Physical and chemical studies on concanavalin A, the hemagglutinin of the jack bean. Arch Biochem Biophys. 1968; 124:218–29. [PubMed: 5661602]
79. Pace CN, Vajdos F, Fee L, Grimsley G, Gray T. How to measure and predict the molar absorption coefficient of a protein. Protein Sci. 1995; 4:2411–2423. [PubMed: 8563639]
80. Blanco M, Coello J, Iturriaga H, Maspoch S, Redón M. Principal component regression for mixture resolution in control analysis by UV-visible spectrophotometry. Appl Spectrosc. 1994; 48:37–43.
81. Harvey DJ. Postsource decay fragmentation of N-linked carbohydrates from ovalbumin and related glycoproteins. J Am Soc Mass Spectrom. 2000; 11:572–577. [PubMed: 10833031]
82. Stein PE, Leslie AG, Finch JT, Carrell RW. Crystal structure of uncleaved ovalbumin at 1.95 A resolution. J Mol Biol. 1991; 221:941–59. [PubMed: 1942038]
83. Bujacz A. Structures of bovine, equine and leporine serum albumin. Acta Crystallogr D Biol Crystallogr. 2012; 68:1278–89. [PubMed: 22993082]
84. Mine Y, Noutomi T, Haga N. Emulsifying and structural properties of ovalbumin. J Agric Food Chem. 1991; 39:443–446.
85. Monkos K. Viscosity analysis of the temperature dependence of the solution conformation of ovalbumin. Biophys Chem. 2000; 85:7–16. [PubMed: 10885394]

86. Tsai D-H, DelRio FW, Keene AM, Tyner KM, MacCuspie RI, Cho TJ, Zachariah MR, Hackley VA. Adsorption and conformation of serum albumin protein on gold nanoparticles investigated using dimensional measurements and in situ spectroscopic methods. Langmuir. 2011; 27:2464–2477. [PubMed: 21341776]

87. Ianeselli L, Zhang F, Skoda MWA, Jacobs RMJ, Martin RA, Callow S, Prévost S, Schreiber F. Protein-protein interactions in ovalbumin solutions studied by small-angle scattering: Effect of ionic strength and the chemical nature of cations. J Phys Chem B. 2010; 114:3776–3783. [PubMed: 20192264]

88. Jungbauer A, Machold C, Hahn R. Hydrophobic interaction chromatography of proteins: III. Unfolding of proteins upon adsorption. J Chromatogr A. 2005; 1079:221–228. [PubMed: 16038308]

89. Kondo A, Oku S, Higashitani K. Structural changes in protein molecules adsorbed on ultrafine silica particles. J Colloid Interface Sci. 1991; 143:214–221.

***Highlights**

- Developed lectin - modified nanoporous gold monolith for separation and extraction of glycoproteins.
- Thermogravimetric analysis used to determine the surface coverage on the monoliths.
- UV detection for in situ determination of the surface coverage on the nanoporous gold monoliths.
- Con A-modified nanoporous gold shows selectivity for capture of ovalbumin.
- Bound ovalbumin eluted using the competitive ligand α-methyl mannopyranoside.

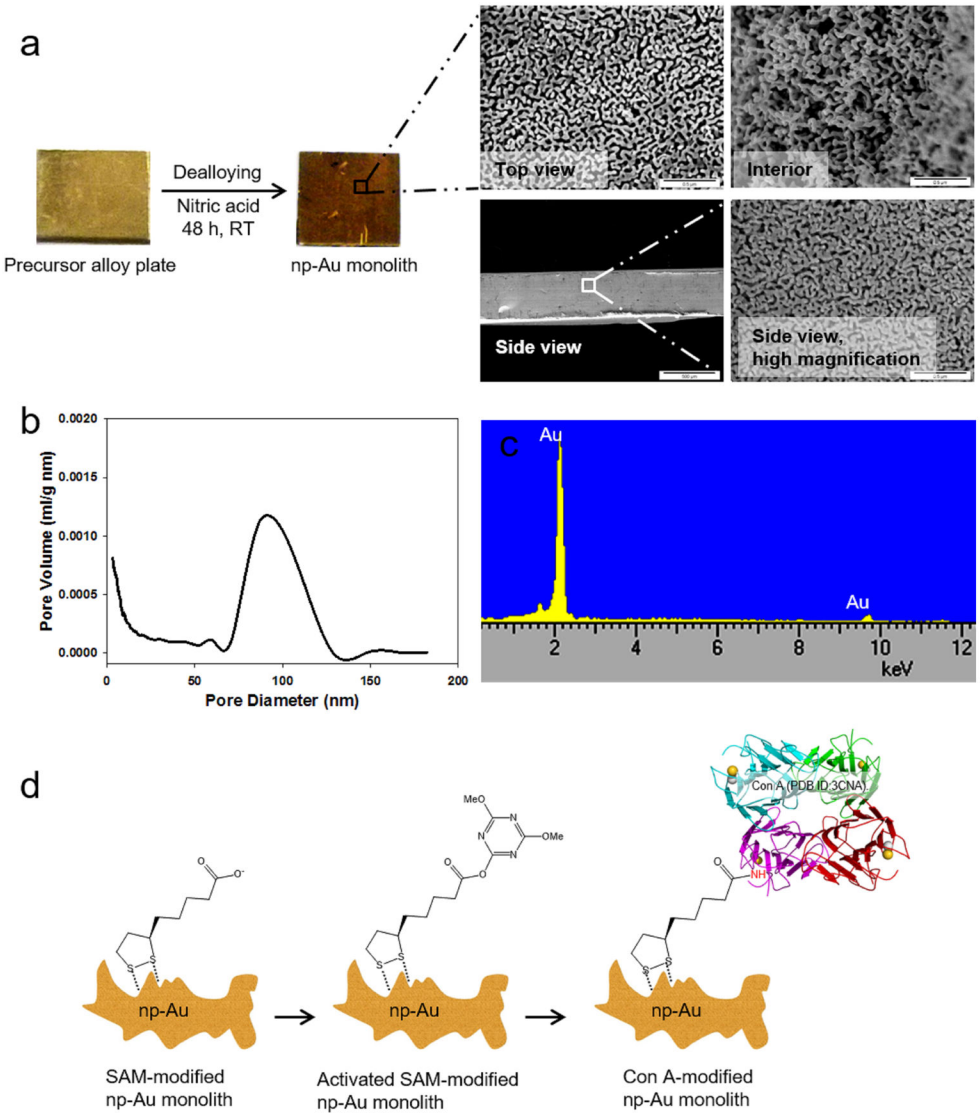

Fig. 1.

(a) Preparation of np-Au monolith from a precursor alloy plate (42% Au, 20% Ag, 38% Cu) through dealloying in nitric acid solution for 48 h at room temperature (RT). SEM images of the top and side views of the exterior and the interior portion of an 8 mm × 8 mm × 0.50 mm np-Au monolith. All scale bars are 0.5 μm except for the side view (left image) which is 500 μm. (b) Pore size distribution obtained by Barrett–Joyner–Halenda (BJH) analysis of the adsorption branch of the isotherm. (c) EDS spectra of np-Au monolith (at 15 kV). (d) Schematic diagram of the preparation of Con A-modified np-Au monolith.

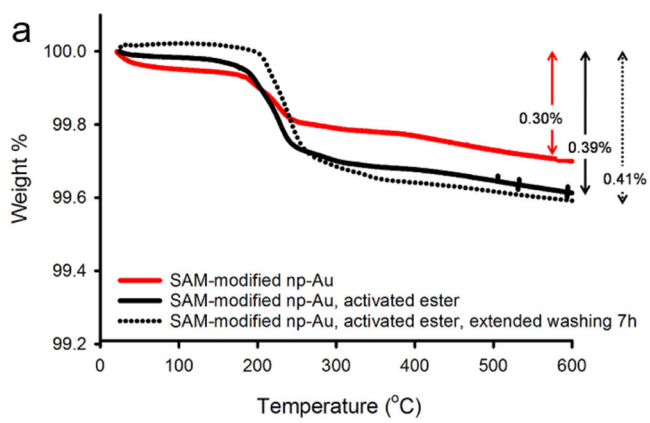

	Wt. Change (%)	Mass loss (mg m^{-2})
SAM-modified np-Au	0.30	0.4485 ± 0.0366
SAM-modified np-Au, activated	0.39	0.5796 ± 0.0474
SAM-modified np-Au, activated (extended washing 7h)	0.41	0.6117 ± 0.0500

Molecules LA immobilized per m^2 np-Au = 1.31×10^{18}

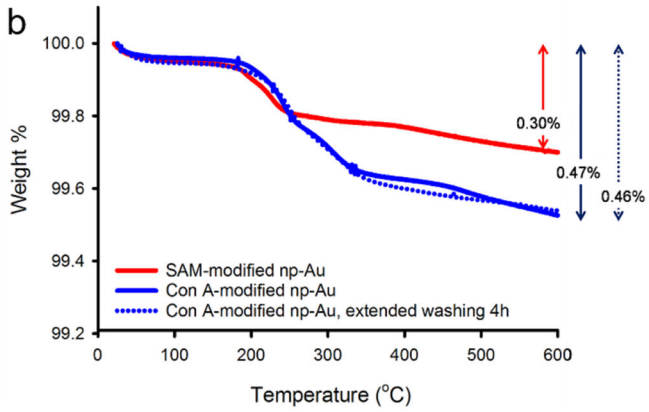

	Wt. Change (%)	Mass loss (mg m^{-2})
SAM-modified np-Au	0.30	0.4485 ± 0.0366
Con A-modified np-Au	0.47	0.7098 ± 0.0580
Con A-modified np-Au (extended washing 4h)	0.46	0.6920 ± 0.0565

Molecules Con A immobilized per m^2 np-Au = 1.85×10^{15}

Fig. 2.

(a) TGA thermograms for determination of LA loading and stability on np-Au monolith. (b) TGA thermograms for determination of Con A loading and stability on SAM-modified np-Au monolith. The temperature was ramped at 20 °C min^{-1}.

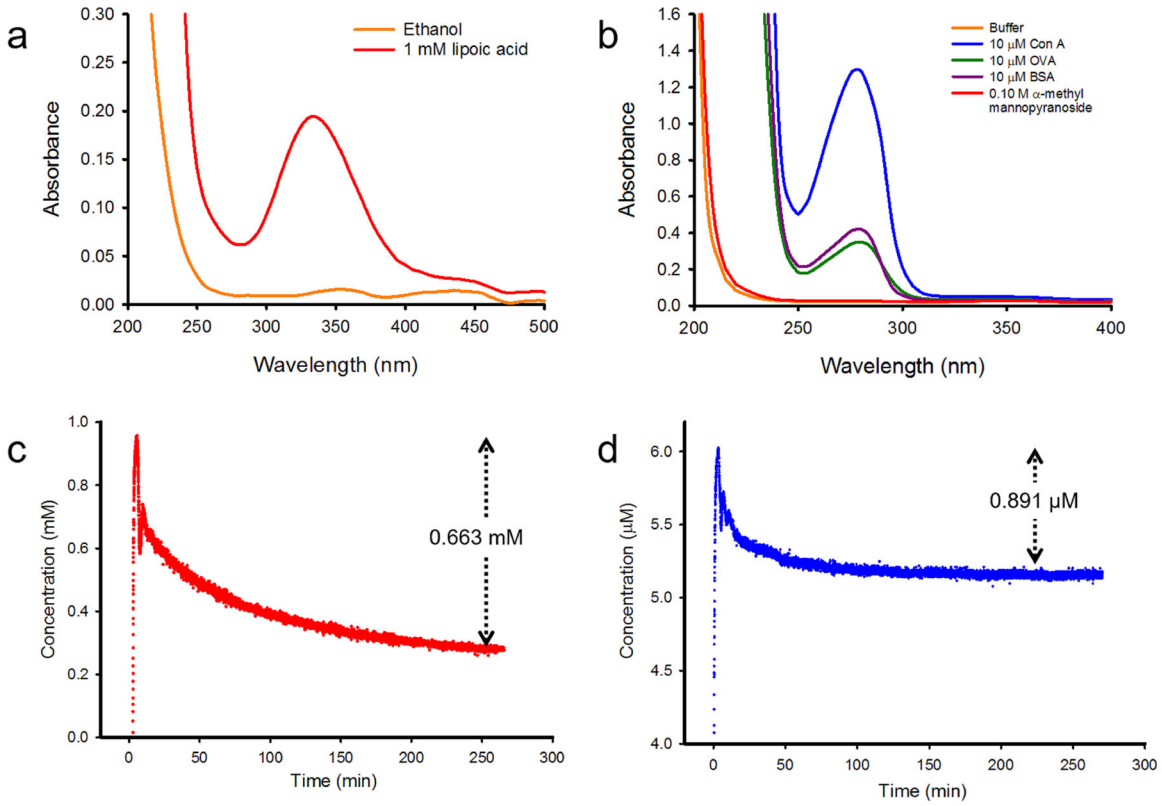

Fig. 3.

(a) UV-vis scan of LA solution. (b) UV-vis scans of protein solutions. (c) Loading curve of LA on np-Au monolith and (d) of Con A on SAM-modified np-Au monolith as recorded by a UV detector at 330 nm and 280 nm, respectively.

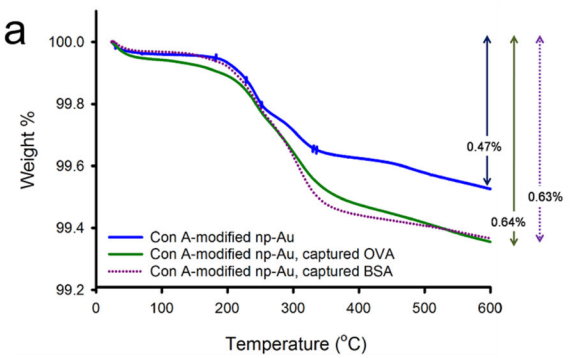

	Wt. Change (%)	Mass loss (mg m^{-2})
Con A-modified np-Au	0.47	0.7098 ± 0.0580
Con A-modified np-Au, captured OVA	0.64	0.9680 ± 0.0791
Con A-modified np-Au, captured BSA	0.63	0.9514 ± 0.0777

Molecules OVA captured per m^2 np-Au = 4.21 x 10^{15}

Molecules BSA captured per m^2 np-Au = 2.63 x 10^{15}

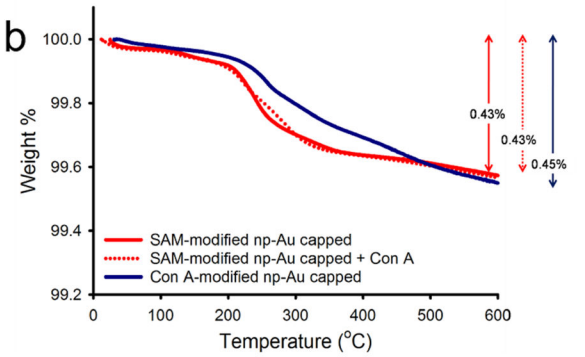

	Wt. Change (%)	Mass loss (mg m^{-2})
SAM-modified np-Au capped	0.43	0.6401 ± 0.0523
SAM-modified np-Au capped + Con A	0.43	0.6501 ± 0.0531
Con A-modified np-Au capped	0.45	0.6745 ± 0.0551

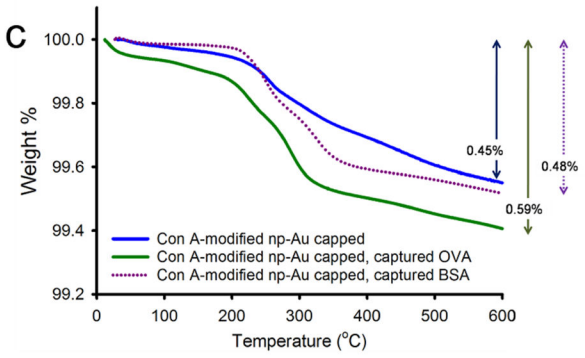

	Wt. Change (%)	Mass loss (mg m^{-2})
Con A-modified np-Au capped	0.45	0.6745 ± 0.0551
Con A modified np-Au capped, captured OVA	0.59	0.8895 ± 0.0727
Con A modified np-Au capped, captured BSA	0.48	0.7235 ± 0.0591

Molecules OVA captured per m^2 np-Au = 3.51 x 10^{15}

Molecules BSA captured per m^2 np-Au = 0.533 x 10^{15}

Fig. 4.

(a) TGA thermograms showing the capture of OVA and BSA using Con A-modified np-Au monolith without the capping procedure. (b) TGA thermograms showing the effect of adding the capping procedure i.e., immobilization of Con A to the esters of SAM modified np-Au monolith was restricted by the capping procedure. (c) TGA thermograms showing the capture of OVA and BSA using Con A-modified np-Au monolith with capping procedure. The temperature was ramped at 20 °C min^{-1}.

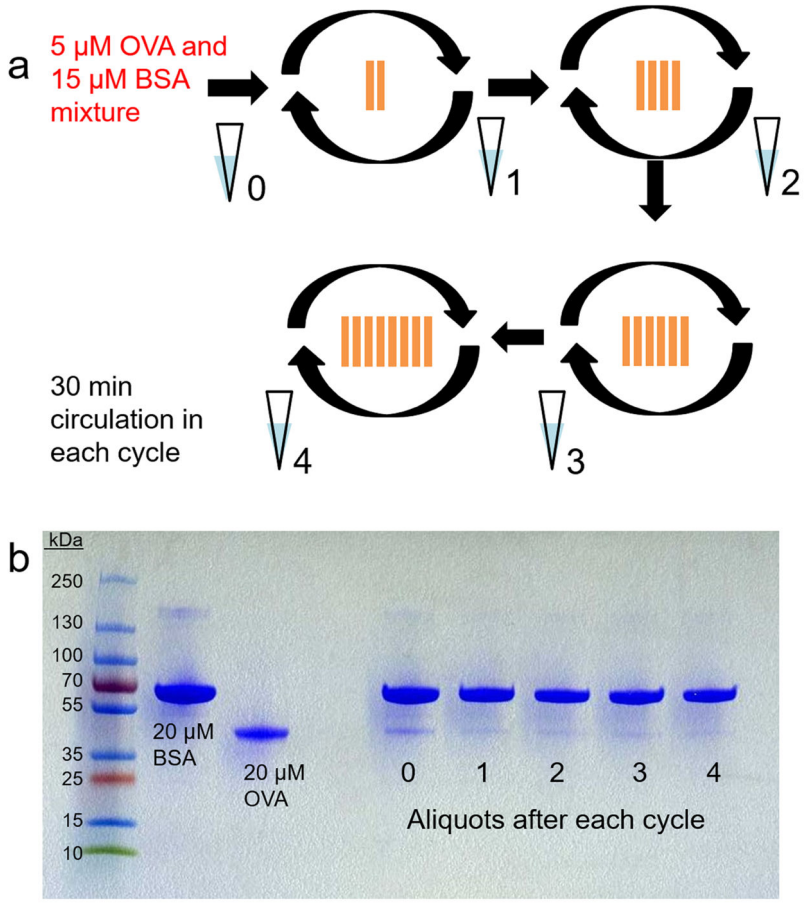

Fig. 5.

(a) Schematic diagram of the procedure used in characterizing extraction of OVA from a mixture with BSA using Con A-modified np-Au monoliths. (b) SDS-PAGE of 20 μM BSA (66.4 kDa) and 20 μM OVA (44.3 kDa) and of the aliquots obtained at the end of each 30 min cycle of circulation of 1:3 molar mixture of OVA and BSA through an increasing number of Con A-modified np-Au monoliths.

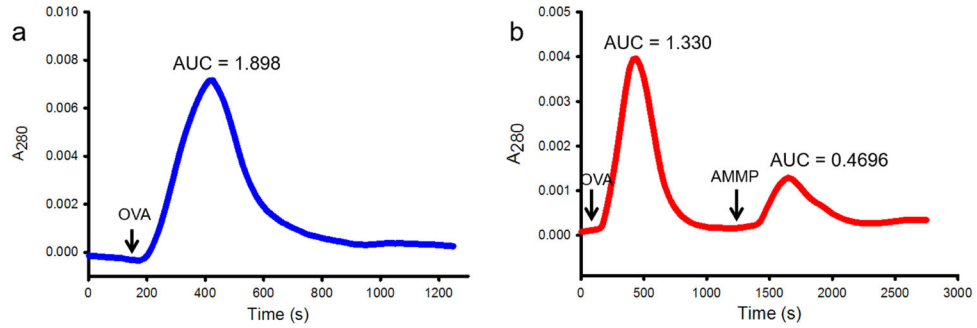

Fig. 6.

(a) Chromatogram generated by flowing 2 mL 1 μM OVA solution through the flow cell without the np-Au monolith. (b) Chromatogram generated by flowing 2 mL 1 μM OVA solution through the Con A-modified np-Au monolith followed by elution using 2 mL 0.1 M α-methyl mannopyranoside (AMMP). AUCs were calculated using GraphPad Prism 6.07.